Journal of Sound and Vibration (2000) **230**(5), 1009–1030
doi:10.1006/jsvi.1999.2454, available online at http://www.idealibrary.com on IDEAL®

COMPARISON OF NATURAL FREQUENCIES OF LAMINATES BY 3-D THEORY, PART II: CURVED PANELS

YEONG-CHYUAN CHERN

Department of Mechanical Engineering, National Chin Yi Institute of Technology, Taichung, Taiwan 411, *R.O.C.*

AND

C. C. CHAO

Department of Power Mechanical Engineering, National Tsing Hua University, Hsinchu, Taiwan 300, *R.O.C.*

(*Received* 19 *August* 1998, *and in final form* 11 *June* 1999)

A three-dimensional vibration study is presented using the three-dimensional theory developed by Chao *et al.* [34–39] for a variety of simply supported shallow spherical, cylindrical, plate, and saddle (hyberbolic) panels in rectangular planform. A complete survey and comparison of existing literature have been made with excellent lowest frequencies via a 3-D augmented energy variational approach. In all of these shell configurations, natural frequencies are noted to decrease in the above-mentioned order according to minimum total potential energy in the natural state.

1. INTRODUCTION

There are numerous papers published on vibration of shells and shallow panels. The present work is a general survey of and comparison with the literature focused on free vibration of the various curved panels, isotropic [1–5, 7–9] and laminated composite [10–42], on simple supports. The most commonly studied geometric configurations are of the cylindrical and spherical types of construction, but there are a few of the hyperbolic or saddle shapes [5, 41]. As to composites lamination, most are reported on cross-ply with a few on angle-ply constructions [6, 14, 19, 23, 28, 40]. Fundamental theories have been evolving through the classical shell theory [1–4, 6–9, 26], first order shear deformation theory (FSDT) [5, 10–21], and higher order shear deformation theory (HSDT) [22–25, 27–28]. Numerical methods include finite elements [4, 9, 13, 15–18, 31], B spline functions and finite strips [7–9, 19, 20, 28], and boundary domain elements [21]. In recent years, there has been strong tendency to pursue the three-dimensional analysis [29–42] on more rigorous grounds.

To start with free vibration of the isotropic curved panels, fundamentals frequencies of aluminium cylindrical panels were studied by Deb Nath [1] in 1969.

0022-460X/00/101009 + 22 $35.00/0

Formulas for natural frequency and mode shape were also available in Belvins [2] and Soedel [3] for the linear classical thin shell theory. The results were checked again by Bardell and Mead [4] by use of the hierarchical finite element method with displacement fields in Legendre polynomials. Kobayashi and Leissa [5] solved the non-linear problem of large-amplitude free vibration of thick shallow shells using the FSDT and Galerkin's procedure. By using the B spline function, the associated finite strip, and finite element analysis, Shen and Wan [7], Geannakakes and Wang [8], and Fan and Luah [9] performed a series of vibration analyses of spherical and cylindrical shell panels.

Secondly, a general review and comparison is made on laminated shell panels. Vibration and buckling of cross-ply laminated circular cylindrical panels were discussed in the early work of Sinha and Rath [10]. Bert and Kumar [11] analyzed the vibration of cylindrical shells of bimodulus composite materials on a shear deformation basis. Reddy [12] obtained a solution for fundamental frequencies of moderately thick laminated cylindrical and spherical shells by using the first order shear deformation theory with a shear correction factor. Finite element analyses for free vibration natural frequencies of cross-ply laminated cylindrical panels were performed by Fong [13], Ganapathi *et al.* [15], Chakravorty *et al.* [16, 17], Goswami and Mukhopadhyay [18], and a spline strip analysis of Mizusawa and Kito [20], based on FSDT. Natural frequencies of antisymmetric angle-ply laminated circular cylindrical panels were also reported by Soldatos [6] using the classical shell theory and Galerkin method, by Kabir and Chaudhuri [14] using FSDT, and by Mizusawa and Kito [19] using the spline strip method. Wang and Schweizerhof [21] established the boundary-domain element method for free vibration of moderately thick laminated orthotropic shallow shells in which a shear correction factor of $\frac{5}{6}$ was also used.

The higher order shear deformation theory HSDT was developed by Reddy and Liu [22] for shells laminated in orthotropic layers by setting shear stress free on the lateral surfaces without regard to transverse normal stress condition and the interlaminar transverse stress continuity. Bending and frequencies were treated for cross-ply cylindrical and spherical shell panels. Soldatos [23] discussed the influence of thickness shear deformation on free vibrations of rectangular plates, cylindrical panels and cylinders of antisymmetric angle-ply construction. Librescu *et al.* [24], and Palazotto and Linnemann [25] investigated free vibration and buckling of laminated composite shallow shell-type panels using HSDT. A three-dimensional version for vibration and stability studies on simply supported cross-ply doubly curved shells was proposed by Wu *et al.* [27] in terms of conventional stress resultants and stress couples.

In three-dimensional analysis, Bhimaraddi [29] investigated the free vibration of doubly curved shallow shells in rectangular planform with interface continuity of three-dimensional displacements and transverse stresses without considering the Poisson strain effects. Analytical solutions for three-dimensional deformation, stress and free vibration of thick, doubly curved, laminated shells were obtained by Fan and Zhang [30]. Beakou and Touratier [31] developed a rectangular finite element for analyzing composite multilayered shallow shells in statics, vibration and buckling with interface continuity and lateral surface conditions of transverse

shear stresses represented by cosine functions without regard to the interfacial transverse normal stress. Ye and Soldatos [32] discussed three-dimensional vibration of laminated cylinders and cylindrical panels with symmetric and antisymmetric cross-ply lay-up using likewise 3-D surface conditions and interface continuity. In general, the difficulty in applying the three-dimensional theory lies in the unavailability of proper three-dimensional material mechanical properties. Philippidis [33] found a way to calculate the transverse Poisson's ratio in fiber reinforced laminae by means of a hybrid experimental approach. The three-dimensional consistent higher order theory has been developed by Chao *et al.* [34–39] with successful application to stress, vibration, impact and shock of the laminated plates and shell panels. Emphasis is placed on consistence with the three-dimensional boundary condition and interlaminar stress continuity, exterior and interior, respectively, as shown in equations (1)–(5), of which no existing literature has taken into full account. Satisfaction of these complicated conditions of the real physical world are implemented by effective use of the higher order displacement fields and Lagrange multipliers via a 3-D augmented energy variational approach. A layer wise analysis for free vibration of thick composite cylindrical shells was done by Huang and Dasgupta [40] by using characteristic beam functions in the in-plane directions and quadratic finite element interpolation in the thickness direction. In the mean time, Huang [41] reported an exact analysis for three-dimensional free vibrations of cross-ply cylindrical and double curved laminates using the 3-D equations of motion and power-series method. Wu *et al.* [42] published their refined asymptotic theory, in which slightly increased frequencies appeared when expanded to order four.

In the present study, a thorough analysis and survey of doubly curved shallow shell panels, including cylindrical, spherical and saddle forms made up of symmetric or antisymmetric, cross-ply or angle-ply lay-ups is made in the essence of three-dimensional elasticity as compared to the literature. The natural frequencies obtained in the numerical analysis are among the lowest known in the literature, because of the thorough consideration given to the three-dimensional boundary conditions and interlaminar continuity to meet the physical requirements of the natural state.

2. THEORETICAL FORMULATION

Consider a K layered curved panel of arc lengths a, b and thickness h with simple supports. In the treatment of the various problems of interest, it may pertain to any one of the following three types of boundary conditions, in which local stresses and displacements are discussed rather than the global stress resultants and stress couples in the conventional theories of plates and shells.

2.1. THREE-DIMENSIONAL BOUNDARY AND INTERLAMINAR CONDITIONS

The conventional edge boundary conditions are modified in the essence of three-dimensional elasticity in terms of local displacements and stresses for the

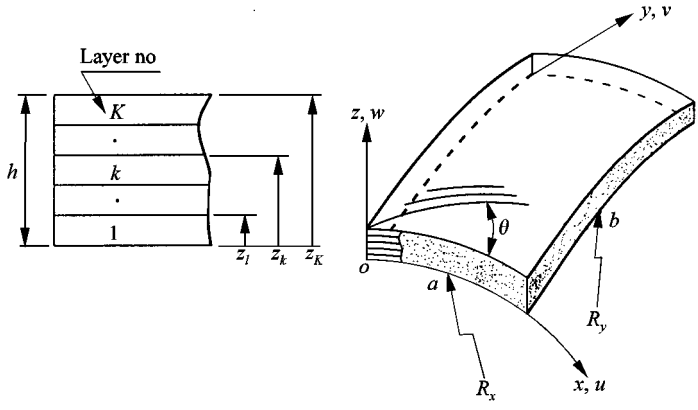

Figure 1. Schematic of laminated curved panels.

various support configurations for the 3-D boundary conditions as shown in equations (1)–(4). In the present study of free vibration, the entire laminated panel is considered surface traction free over both lateral surfaces. Both the natural and geometrical edge conditions are justified by admissible displacement functions exactly everywhere over the four edges for cross-ply laminations, while specified geometric edge conditions are justified for angle-ply and other laminations. Three types of simply supported edge boundary conditions are treated.

Lateral surface traction free conditions:

$$z = 0: \quad \mathscr{F}_1^{(0)} = \sigma_{xz} = 0, \qquad \mathscr{F}_2^{(0)} = \sigma_{yz} = 0, \qquad \mathscr{F}_3^{(0)} = \sigma_{zz} = 0,$$

$$z = h: \quad \mathscr{F}_1^{(K)} = \sigma_{xz} = 0, \qquad \mathscr{F}_2^{(K)} = \sigma_{yz} = 0, \qquad \mathscr{F}_3^{(K)} = \sigma_{zz} = 0, \tag{1}$$

S_1 *fixed pin supported edges*:

$$x = 0, a: \quad z = 0, \qquad \sigma_{xx} = u = v = w = 0; \qquad z \neq 0, \quad \sigma_{xx} = v = w = 0,$$

$$y = 0, b: \quad z = 0, \qquad \sigma_{yy} = u = v = w = 0; \qquad z \neq 0, \quad \sigma_{yy} = u = w = 0, \tag{2}$$

S_2 *higher-roller support edges*:

$$x = 0, a: \quad \sigma_{xx} = v = w = 0; \qquad y = 0, b: \qquad \sigma_{yy} = u = w = 0. \tag{3}$$

S_3 *sliding pin supported edges*:

$$z = 0, \quad x = 0, a: \quad \sigma_{xy} = u = w = 0; \qquad y = 0, b: \quad \sigma_{yx} = v = w = 0. \tag{4}$$

The surface conditions are labelled as $\mathscr{F}_i^{(0)}$ and $\mathscr{F}_i^{(K)}$ for transverse normal and shear stresses free at the bottom and top surface respectively. Pasternak or Winkler mode elastic foundation may be incorporated into the surface condition if required.

Interlaminar continuity: Since individual displacement fields are assumed for each layer of the laminate, interlaminar continuity of layer displacements in

addition to transverse stresses must be satisfied at each interface between adjacent layers:

$$\mathscr{F}_1^{(k)} = \sigma_{xz}^{(k)^+} - \sigma_{xz}^{(k+1)^-} = 0, \qquad \mathscr{F}_4^{(k)} = u^{(k)^+} - u^{(k+1)^-} = 0,$$
$$\mathscr{F}_2^{(k)} = \sigma_{yz}^{(k)^+} - \sigma_{yz}^{(k+1)^-} = 0, \qquad \mathscr{F}_5^{(k)} = v^{(k)^+} - v^{(k+1)^-} = 0,$$
$$\mathscr{F}_3^{(k)} = \sigma_{zz}^{(k)^+} - \sigma_{zz}^{(k+1)^-} = 0, \qquad \mathscr{F}_6^{(k)} = w^{(k)^+} - w^{(k+1)^-} = 0,$$
$$k = 1, 2, \ldots, K-1, \tag{5}$$

where, for simplicity, the interlaminar conditions are denoted as $\mathscr{F}_i^{(k)}$ with subscripts 1, 2, 3, for the transverse stresses σ_{xz}, σ_{yz}, σ_{zz} and 4, 5, 6 for layer displacement u, v, w. The superscripts $+$ and $-$ denote the upper and lower surface of the respective layers. Layers are numbered from the bottom upwards.

2.2. THREE-DIMENSIONAL DISPLACEMENT FIELDS

Three-dimensional displacement fields are assumed according to the various edge boundary conditions as above for each layer in terms of double Fourier series of x, y for the in-plane co-ordinates and polynomials in z to proper higher orders for the out-of-plane co-ordinate,

S_1 fixed pin displacement field:

$$u^k(x, y, z, t) = \sum_1^J \sum_1^M \sum_0^N U_{jmn}\, z^j \sin x_m \cos y_n,$$
$$v^k(x, y, z, t) = \sum_1^J \sum_1^M \sum_0^N V_{jmn}\, z^j \sin x_m \cos y_n,$$
$$w^k(x, y, z, t) = \sum_0^J \sum_1^M \sum_1^N W_{jmn}\, z^j \sin x_m \sin y_n, \tag{6}$$

where $x_m = m\pi x/a, \quad y_n = n\pi y/b.$

S_2 hinge-roller displacement field:

$$u^k(x, y, z, t) = \sum_0^M \sum_1^N \left[U_{0mn}\left(1 + \frac{z}{R_x}\right) + \sum_1^J U_{jmn} z^j \right] \cos x_m \sin y_n,$$
$$v^k(x, y, z, t) = \sum_1^M \sum_0^N \left[V_{0mn}\left(1 + \frac{z}{R_y}\right) + \sum_1^J V_{jmn} z^j \right] \sin x_m \cos y_n,$$
$$w^k(x, y, z, t) = \sum_0^J \sum_1^M \sum_1^N W_{jmn}\, z^j \sin\, x_m \sin y_n. \tag{7}$$

S_3 sliding pin displacement field:

$$u^k(x, y, z, t) = \sum_1^M \sum_0^N U_{0mn}\left(1 + \frac{z}{R_x}\right) \sin x_m \cos y_n + \sum_1^J \sum_0^M \sum_1^N U_{jmn} z^j \cos x_m \sin y_n,$$

$$v^k(x, y, z, t) = \sum_0^M \sum_1^N V_{0mn}\left(1 + \frac{z}{R_y}\right)\cos x_m \sin y_n + \sum_1^J \sum_1^M \sum_0^N V_{jmn} z^j \sin x_m \cos y_n,$$

$$w^k(x, y, z, t) = \sum_0^J \sum_1^M \sum_1^N W_{jmn} z^j \sin x_m \sin y_n. \tag{8}$$

2.3. THREE-DIMENSIONAL ENERGY VARIATIONAL APPROACH

Strain components in a layer: In accordance with the three-dimensional shell theory [34, 37], the small strains are expressed in terms of the displacement

$$\varepsilon_{xx} = \frac{1}{1 + z/R_x}\left(\frac{\partial u}{\partial x} + \frac{w}{R_x}\right), \qquad \gamma_{xz} = \frac{1}{1 + z/R_x}\left(\frac{\partial w}{\partial x} - \frac{u}{R_x}\right) + \frac{\partial u}{\partial z},$$

$$\varepsilon_{yy} = \frac{1}{1 + z/R_y}\left(\frac{\partial v}{\partial y} + \frac{w}{R_y}\right), \qquad \gamma_{yz} = \frac{1}{1 + z/R_y}\left(\frac{\partial w}{\partial y} - \frac{v}{R_y}\right) + \frac{\partial v}{\partial z},$$

$$\varepsilon_{zz} = \frac{\partial w}{\partial z}, \qquad \gamma_{xy} = \frac{1}{1 + z/R_y}\frac{\partial u}{\partial y} + \frac{1}{1 + z/R_x}\frac{\partial v}{\partial x}, \tag{9}$$

where R_x and R_y denote the principle radii of curvature of the curved panel in the x and y directions respectively. Influence of the double curvatures has been considered in corresponding terms in the above equations.

Stress components in a layer: The three-dimensional stresses in the shell panels are obtained by using the anisotropic constitutive law of composites. In most of the numerical examples in the referenced literature, the 3-D property data were incomplete. The v_{23}^p can be calculated as per equation (13) in reference [33] and the transverse shear modulus $G_{23} = E_2/[2(1 + v_{23}^p)]$.

$$\begin{Bmatrix} \sigma_{xx} \\ \sigma_{yy} \\ \sigma_{zz} \\ \sigma_{yz} \\ \sigma_{xz} \\ \sigma_{xy} \end{Bmatrix} = \begin{Bmatrix} \bar{C}_{11} & \bar{C}_{12} & \bar{C}_{13} & 0 & 0 & \bar{C}_{16} \\ \bar{C}_{12} & \bar{C}_{22} & \bar{C}_{23} & 0 & 0 & \bar{C}_{26} \\ \bar{C}_{13} & \bar{C}_{23} & \bar{C}_{33} & 0 & 0 & \bar{C}_{36} \\ 0 & 0 & 0 & \bar{C}_{44} & \bar{C}_{45} & 0 \\ 0 & 0 & 0 & \bar{C}_{45} & \bar{C}_{55} & 0 \\ \bar{C}_{16} & \bar{C}_{26} & \bar{C}_{36} & 0 & 0 & \bar{C}_{66} \end{Bmatrix} \begin{Bmatrix} \varepsilon_{xx} \\ \varepsilon_{yy} \\ \varepsilon_{zz} \\ \gamma_{yz} \\ \gamma_{xz} \\ \gamma_{xy} \end{Bmatrix} \tag{10}$$

Energy formulation: In derivation of the modified equations of motion with the surface conditions and interlaminar continuity included via a 3-D augmented energy variational approach, the total potential is composed of the strain energy, kinetic energy, and the above-mentioned constraints enforced by the use of Lagrange multipliers.

$$V = \sum_{k=1}^K \int_{v_k} \left\{\frac{1}{2}\,\sigma_{ij}\,\varepsilon_{ij}\right\}_k \left(1 + \frac{z}{R_x}\right)\left(1 + \frac{z}{R_y}\right) \mathrm{d}x\,\mathrm{d}y\,\mathrm{d}z, \quad i, j = x, y, z,$$

$$T = \sum_{k=1}^K \int_{v_k} \left\{\frac{1}{2}\,\rho(u_{,t}^2 + v_{,t}^2 + w_{,t}^2)\right\}_k \left(1 + \frac{z}{R_x}\right)\left(1 + \frac{z}{R_y}\right) \mathrm{d}x\,\mathrm{d}y\,\mathrm{d}z,$$

$$SC = \sum_{k=0,\,K} \sum_{i=1}^{3} \int_{S_k} \{\lambda_i^{(k)} \mathscr{F}_i^{(k)}\} \left(1 + \frac{z_k}{R_x}\right)\left(1 + \frac{z_k}{R_y}\right) \mathrm{d}x\,\mathrm{d}y,$$

$$IC = \sum_{k=1}^{K-1} \sum_{i=1}^{6} \int_{S_k} \{\lambda_i^{(k)} \mathscr{F}_i^{(k)}\} \left(1 + \frac{z_k}{R_x}\right)\left(1 + \frac{z_k}{R_y}\right) \mathrm{d}x\,\mathrm{d}y,$$

$$\Pi = V - T + SC + IC. \tag{11}$$

Modified Lagrange's equations: The three-dimensional displacement can be partitioned into the lower- and higher-order parts denoted by vectors U_l and U_h, namely,

$$\{U\}^{\mathrm{T}} = \{U_l \,|\, U_h\}^{\mathrm{T}},$$

$$\{U_l\}^{\mathrm{T}} = \{U_{jmn},\, V_{jmn},\, W_{jmn}\}^{\mathrm{T}}, \quad j = 1, 2, \ldots, J-2,$$

$$\{U_h\}^{\mathrm{T}} = \{U_{jmn},\, V_{jmn},\, W_{jmn}\}^{\mathrm{T}}, \quad j = J-1, J. \tag{12}$$

Using the lateral surface and interlaminar constraint conditions as above, the six degrees of freedom of the higher order part can be eliminated in each layer for each Fourier series component. A system of modified Lagrange's equations of motion is obtained via energy variation with respect to the generalized displacements and Lagrange multipliers:

$$\frac{\partial \Pi}{\partial \lambda_i} = 0 \;\Rightarrow\; [L_\lambda^h]\,\{U_h\} = -[L_\lambda^\ell]\,\{U_\ell\},$$

$$\frac{\partial \Pi}{\partial U_i} = 0 \;\Rightarrow\; [M]\,\{\ddot{U}\} + [K]\,\{U\} + [L_\lambda^T]\,\{\Lambda\} = \{0\}, \tag{13}$$

where $[L_\lambda]$ is a matrix representing the surface and interlaminar continuity relationship with $[L_\lambda^\ell]$ and $[L_\lambda^h]$ as submatrices through partitioning. $[M]$ and $[K]$ are the mass and stiffness matrices of the system, which can be converted to reduced forms by use of the lower order displacement alone.

Assuming simple harmonic motion in free vibration, the following eigenvalue problem is derived:

$$[\bar{K}]\,\{U_\ell\} = \omega^2\,[\bar{M}]\,\{U_\ell\}, \tag{14}$$

where ω is the natural frequency of the free vibration.

3. RESULTS AND DISCUSSION

By use of the present three-dimensional theory of laminated shells, a generally survey is made in this work focusing on free vibration of the various simply supported curved panels of rectangular planform. Numerical results are compared with other results in the literature in the order of isotropic and laminated composites, cross-ply and angle-ply in the cylindrical, spherical and hyperbolic configurations. Different displacement fields are used for different boundary conditions as the case pertains to. Basically, the concepts of constant or averaged transverse shear of the FSDT, and the parabolic transverse shear distribution of the

HSDT are inconsistent with real physics to account for three-dimensional boundary conditions of no surface traction in free vibration and the interface continuity of displacements and transverse stresses. The present theory are rigorous in that all these conditions are taken into consideration through a 3-D augmented energy as variational approach in persuit of a natural state for minimum potential energy as required in the theory of elasticity. As a result, all natural frequencies obtained in the present study are almost the lowest among all other results in the literature, with few exception bearing an $*$ marks which will be accounted for when it occurs.

3.1. ISOTROPIC CURVED PANELS

Firstly, consider several isotropic aluminum alloy cylindrical panels of axial length $a = 27{\cdot}94$ cm and arc length $b = 22{\cdot}86$ cm. The present results give the lowest frequencies as compared against Deb Nath [1], Bardell and Mead [4], and calculated values from Soedel [3] as shown in Table 1.

Natural frequencies of the first ten/twelve modes of the isotropic cylindrical/spherical curved panels of square planform are shown in Table 2 in comparison with the results of Shen and Wan [7], Geannakakes and Wang [8], Fan and Luah [9], and values calculated as per Blevins [2]. In this case study, the S_2 hinge-roller support displacement fields are adopted. Two frequencies in reference [8] using B_3-spline finite strips in the classical thin shell theory with exact curvatures incorporated in the in-plane normal strains are found to be slightly lower in the case of cylindrical panels. Otherwise, the present results yield the lowest frequencies of all

Various isotropic shells: Table 3 shows the fundamental frequencies of various isotropic shell panels as compared to Kobayashi and Leissa [5], in which larger amplitude vibrations were investigated on a non-linear FSDT basis using shear correction factor $\kappa = \frac{5}{6}$. Case studies include spherical and saddle panels of square and rectangular plan forms for various thicknesses and radius parameters. Also studied are thin to thick spherical and cylindrical panels versus aspect ratio b/a.

TABLE 1

Lowest frequencies ω_{mn} of aluminum cylindrical panels, Hz

R (cm)	h (cm)	m, n	Ref. [1]	[3]	[4]	S_2
243·84	0·07112	1,1	144·5	143·8	144·3	142·1
243·84	0·12190	1,1	163·9	163·1	163·7	161·4
182·88	0·07112	1,2	167·8	167·2	167·8	166·7
182·88	0·12190	1,1	201·7	200·8	201·4	198·5
121·92	0·07112	1,2	182·2	181·6	182·1	180·8
121·92	0·12190	1,2	282·3	281·8	282·5	278·1

7075 T-6: $E = 72$ GPa, $\nu = 1/3$, $\rho = 2{\cdot}8$ g/cm^3.

TABLE 2

Natural frequencies ω_{mn} of isotropic curved shell panels, rad/s

Panels	*m,n*	Reference [2]	[7]	[8]	[9]	S_2
Cylindrical	1,1	0·28452	0·28285	0·28220	—	0·28016
	2,1	0·29765	0·30285	0·31593	—	0·29214
	2,2	0·51697	0·50551	0·49745*	—	0·49846
	3,1	0·55969	0·52489	0·51843	—	0·50971
	1,2	0·59308	0·57185	0·58479	—	0·54862
	1,3	0·76461	0·73930	0·71976*	—	0·72361
	3,2	0·77026	0·75758	0·75347	—	0·72931
	2,3	0·89381	0·82441	0·80075	—	0·79998
	4,1	0·94781	0·96993	0·97587	—	0·92680
	3,3	1·03663	1·05842	1·05303	—	1·01875
Spherical	1,1	0·53585	0·52835	0·53146	0·53263	0·52543
	1,2	0·59621	0·59151	0·59114	0·59041	0·58420
	2,1	0·59621	0·59253	0·59641	0·59080	0·58487
	2,2	0·69454	0·69040	0·68980	0·68486	0·67676
	1,3	0·77430	0·77070	0·76283	0·76020	0·75219
	3,1	0·77430	0·77307	0·77390	0·76260	0·75220
	2,3	0·90779	0·90372	0·89397	0·89010	0·87811
	3,2	0·90779	0·90744	0·89940	0·89025	0·87804
	4,1	1·10208	1·10283	1·09537	1·07837	1·06234
	1,4	1·10208	1·15263	1·13240	1·07871	1·06018
	3,3	1·15259	—	—	1·12711	1·10792
	2,4	1·25531	—	—	1·22187	1·20342

$E = 1$, $\nu = 0{\cdot}3$, $\rho = 1$, $a = b = 1{\cdot}0118$, $h = 0{\cdot}0191$, $R = 1{\cdot}91$, $L = 1$ (chord).

The present results give the lowest frequencies except for one case of thin spherical shell where a loose discount of $\kappa = \frac{5}{6}$ in their shear modulus was used in the FSDT formulation. It is understood that FSDT might be easier for the complicated non-linear analysis. Henceforth, no specific accounts and comments will be given when lower frequencies reported elsewhere from FSDT or CSD as referred to later in reference [29] for constant shear deformation are listed.

3.2. CROSS-PLY CURVED PANELS

Cylindrical cross-ply: To demonstrate the effect of aspect ratio, the normalized fundamental frequencies of the [0/90] cross-ply cylindrical shell shallow panels of radius $R = 40h$ and arc length $b = 20h$ are listed in Table 4. The present three-dimensional analysis of S_2 reveals the most favourable frequencies in comparison with Sinha and Rath [10], Bert and Kumar [11], Fong [13], Beakou and Touratier [31], and Huang and Dasgupta [40].

The effects of thickness and curvature are considered as follows. In Table 5, normalized fundamental frequencies $\Omega = \omega a^2 (\rho/E_2 h^2)^{1/2}$ are examined versus the

TABLE 3

Fundamental frequencies of isotropic shell panels $\Omega = \omega a[\rho(1-\nu^2)/E]^{1/2}$

1. Spherical			2. Spherical			3. Spherical, $a/h = 10$		
a/h	[5]	S_2	R_x/a	[5]	S_2	b/a	[5]	S_2
5	1·0330	0·99626	10	0·1111	0·11044	0·5	1·3370	1·29904
10	0·5622	0·55250	20	0·07429	0·07222	1.0	0·5622	0·55358
50	0·1485	0·14766	50	0·06007	0·06004	1·5	0·4142	0·40454
100	0·1111	0·11026	100	0·05776	0·05719	2·0	0·3624	0·35023
200	0·09955	0·09912	∞	—	0·05647			
4. Spherical, $a/h = 100$			5. Cylindrical, $a/h = 10$			6. Cylindrical, $a/h = 100$		
b/a	[5]	S_2	b/a	[5]	S_2	b/a	[5]	S_2
0·5	0·1713*	0·18078	0·5	1·3360	1·31742	0·5	0·16150	0·16066
1·0	0·1111	0·11085	1·0	0·5563	0·55049	1·0	0·07429	0·07368
1·5	0·1039	0·08385	1·5	0·4044	0·39987	1·5	0·05053	0·04912
2·0	0·1018	0·06741	2·0	0·3505	0·34612	2·0	0·04039	0·03925
7. Spherical $a/h = 100$			8. Saddle, $a/h = 100$					
R_x/R_y	[5]	S_2	R_x/R_y	[5]	S_2			
0·5	0·09144	0·09087	− 1·0	0·05695	0·05553			
1·0	0·11110	0·11026	− 0·5	0·06174	0·06084			

1. $a = b$, $R_x = R_y$, $R_x/a = 10$; 3,4. $R_x/a = R_y/b = 10$; 7,8. $a = b$, $R_x/a = 10$;
2. $a = b$, $R_x = R_y$, $a/h = 100$; 5,6. $R_x/a = 10$, $R_y = \infty$; 1–8. $E = 1$, $\nu = 0{\cdot}3$, $\rho = 1$.

TABLE 4

Fundamental frequencies $\Omega = \omega b^2(\rho/E_2h^2)^{1/2}$ *of* [0/90] *cylindrical shell panels of shallowness* $\phi = 0{\cdot}5$ *rad*

a/b	Ref. [10]	[11]	[13]	[31]	[40]	S_2
1	11·71	11·65	11·49	11·56	11·46	11·02
2	7·35	7·37	7·26	7·35	7·26	6·57
3	6·58	6·59	6·52	6·58	6·51	5·75
4	6·32	6·33	6·30	6·32	6·27	5·47
5	6·22	6·21	6·19	6·22	6·17	5·36

$E_1/E_2 = 25$, $E_3/E_2 = 1$, $G_{12}/E_2 = G_{13}/E_2 = 0{\cdot}5$, $G_{23}/E_2 = 0{\cdot}2$, $\nu_{12} = \nu_{13} = \nu_{23} = 0{\cdot}25$.

radius-to-axial-length ratio R_y/a for the 2, 3, 4 layered symmetric/antisymmetric thick and thin cross-ply cylindrical shell panels of equal axial length a and arc length b. The limiting case becomes a flat plate. Verification has been made against Reddy [12] and Chakravorty *et al.* [16]. In reference [12], a shear correction factor

TABLE 5

Normalized fundamental frequencies $\Omega = \omega a^2(\rho/E_2h^2)^{1/2}$ *of cross-ply cylindrical shell panels,* $a = b$

Panel	a/h	R_y/a	1	2	3	4	5	10	10^9
[0/90]	10	[12]	9·9865	9·1476	8·9832	8·9301	8·9092	8·8879	8·8998
		S_2	9·5325	9·0283	8·9391	8·9132	8·9041	8·9009	8·9184
		S_2^p	8·9635	8·8460	8·8478	8·8577	8·8667	8·8919	8·9270
	100	[12]	65·474	34·914	24·516	19·509	16·668	11·831	9·6873
		[16]	—	—	24·520	19·522	16·681	11·838	9·6893
		S_2	59·071	31·689	22·439	18·028	15·551	11·424	9·6824
		S_2^p	50·610	27·413	19·690	16·077	14·087	10·899	9·6871
[0/90/0]	10	[12]	13·172	12·438	12·287	12·233	12·207	12·173	12·162
		S_2	12·259	11·683	11·562	11·518	11·498	11·469	11·457
		S_2^p	11·784	11·575	11·524	11·504	11·493	11·475	11·463
	100	[12]	66·583	36·770	27·116	22·709	20·332	16·625	15·183
		[16]	—	—	27·050	22·685	20·324	16·630	15·192
		S_2	60·248	33·761	25·305	21·502	19·475	16·364	15·165
		S_2^p	48·793	28·486	22·238	19·519	18·105	15·991	15·165
$[0/90]_s$	10	[12]	13·128	12·471	12·337	12·289	12·267	12·236	12·226
		S_2	12·240	11·767	11·669	11·634	11·617	11·594	11·585
		S_2^p	11·796	11·663	11·632	11·618	11·611	11·599	11·591
	100	[12]	66·704	36·858	27·173	22·749	20·361	16·634	15·184
		S_2	59·730	33·532	25·168	21·409	19·409	16·344	15·167
		S_2^p	49·126	28·629	22·310	19·558	18·127	15·991	15·167

Same material properties as in Table 4. $\nu_{23}^p = 0{\cdot}572$ for S_2^p.

$\kappa = \frac{5}{6}$ was used. It seems unreasonable to assume all equal the Poisson ratios as in Table 4 in all three dimensions. Therefore, the transverse Poisson's ratio $\nu_{23}^p = 0{\cdot}572$ is calculated as per Philippidis [33].

Also shown in Table 6 are the fundamental frequencies in rad/s for the thick/thin $[0/90]_S$ roller supported cylindrical shell panels with $a = b$, $h = 1{\cdot}0$ in, as compared to Reddy and Liu [22], and Palazotto and Linnemann [25], in which an extremely large value of $\rho = 1{\cdot}0$ slug/in^3 was assumed. Additional computation for density $\rho^! = 1{\cdot}77 \times 10^{-3}$ slug/in^3 has been done for the case of graphite/epoxy.

As another example, Table 7 shows the variations of normalized fundamental frequencies of simply supported cylindrical panels with radius-to-axial-length R_y/a from 1 to 1000. The [0/90], [0/90/0] and $[0/90]_S$ cross-ply laminations have $a = b$, $a/h = 10$ and $R_x = \infty$. Present results are good in comparison with the FSDT study of Mizusawa and Kito [20] ($\kappa = 5/6$), traditional HSDT of Reddy and Liu [22] and Librescu *et al.* [24], and HSDT-based spline strip method of Mizusawa [28].

Spherical cross-ply: The effects of thickness of curvature of cross-ply square spherical panels are discussed in Tables 8–10. To start with the typical thin shells of $a/h = 100$, Table 8 presents a comparison of normalized fundamental frequencies of the thin square planform 2, 3, 4 layered symmetric and antisymmetric cross-ply

TABLE 6

Fundamental frequencies ω of $[0/90]_S$ roller supported cylindrical shell panels, rad/s

a/h	R_y/a	[22]	[25]	S_2	$S_2^!$
10	5	108·4237	108·6415	106·4883	8768·1851
	10	108·0571	108·109	106·3356	8755·6187
	20	107·9655	107·9753	106·2779	8750·5922
	50	107·9655	107·9379	106·2494	8748·7072
100	5	1·86602	1·8697	1·69505	139·4867
	10	1·52416	1·52458	1·47563	121·2655
	20	1·42519	1·42529	1·41362	116·2389
	50	1·39585	1·39623	1·39471	114·9823

$\frac{E_1}{E_2} = 25$ $E_2 = 840$ ksi $\frac{G_{13}}{E_2} = 0{\cdot}5$ $v_{12} = 0{\cdot}25$ $v_{23}^p = 0{\cdot}572$ $\rho = 1{\cdot}0\,\text{slug/in}^3$,

$\frac{E_3}{E_2} = 1$ $\frac{G_{12}}{E_2} = 0{\cdot}5$ $\frac{G_{23}}{E_2} = 0{\cdot}5$ $v_{13} = 0{\cdot}25$ $R_x = \infty$ $\rho^! = 1{\cdot}77 \times 10^{-3}$.

TABLE 7

Fundamental frequencies $\Omega = \omega a^2 (\rho/E_2 h^2)^{1/2}$ of s.s cylindrica panels

Reference	R_y/a	[0/90]	[0/90/0]	$[0/90]_S$	R_y/a	[0/90]	[0/90/0]	$[0/90]_S$
[20]	5	8·9087	12·2082	—	10	8·8883	12·1742	—
[22]		9·0230	11·8500	11·8300		8·9790	11·8000	11·7900
[24]		8·9590	12·0090	12·0130		8·9330	11·9710	11·9770
[28]		9·0234	11·8460	—		8·9792	11·8040	—
S_2		8·7954	11·5007	11·6054		8·8530	11·4630	11·5887
[20]	20	8·8901	12·1657	—	50	8·8951	12·1633	—
[22]		8·9720	11·7900	11·7800		8·9730	11·7900	11·7800
[24]		8·9340	11·9610	11·9680		8·9390	11·9590	11·9650
[28]		8·9725	11·9730	—		8·9734	11·7910	—
S_2		8·8829	11·4535	11·5824		8·9013	11·4508	11·5793
[20]	100	8·8974	12·1633	—	10^3	8·8998	12·1629	—
[22]		8·9750	11·7900	11·7800		8·9760	11·7900	11·7800
[24]		8·9410	11·9580·	11·9650		8·9440	11·9580	11·9650
[28]		8·9746	11·7900	—		8·9760	11·7900	—
S_2		8·9075	11·4504	11·5784		8·9131	11·2503	11·5776
[20]	1	9·9999	13·1719	—				
S_2		8·4686	12·5674	11·8993				

$E_1/E_2 = 25$, $E_3/E_2 = 1$, $G_{12}/E_2 = G_{13}/E_2 = 0{\cdot}5$, $G_{23}/E_2 = 0{\cdot}35$, $v_{12} = v_{13} = 0{\cdot}25$, $v_{23}^p = 0{\cdot}572$

spherical shell panels to Reddy [12] with $\kappa = \frac{5}{6}$, Ganapathi *et al.* [15], Chakravorty *et al.* [17] and Goswami and Mukhopadhyay [18] and Fan and Zhang [30].

For moderate thickness $a/h = 10$, normalized fundamental frequencies of the 2, 3, 4 layered cross-ply square spherical shallow shell panels are shown in Table 9 for

TABLE 8

Normalized fundamental frequencies $\Omega = \omega a^2(\rho/E_2h^2)^{1/2}$ *of cross-ply thin square spherical shell panels,* $a/h = 100$

Panel	R/a	1	2	3	4	5	10	10^9
[0/90]	[12]	125·93	67·362	46·002	35·228	28·825	16·706	9·6873
	[17]	—	—	45·801	35·126	28·778	16·706	9·6893
	[30]	125·93	67·358	45·991	35·229	28·823	16·714	9·6824
	S_2	123·00	65·812	44·962	34·451	28·210	16·426	9·6824
[0/90/0]	[12]	125·99	68·075	47·265	36·971	30·993	20·347	15·183
	[17]	—	—	47·305	36·890	30·963	20·356	15·192
	[30]	125·99	68·061	47·261	36·968	30·991	20·327	15·171
	S_2	123·10	66·598	46·306	36·280	30·466	20·145	15·165
$[0/90]_S$	[15]	126·276	—	47·399	—	31·074	20·385	15·194
	[18]	126·239	68·493	47·529	37·166	—	—	—
	[30]	126·32	68·296	47·417	37·065	31·069	20·366	15·171
	S_2	123·12	66·645	46·341	36·306	30·486	20·152	15·167

$E_1/E_2 = 25$, $E_3/E_2 = 1$, $G_{12}/E_2 = G_{13}/E_2 = 0{\cdot}5$, $G_{23}/E_2 = 0{\cdot}35$, $\nu_{12} = \nu_{13} = \nu_{23} = 0{\cdot}25$

TABLE 9

Normalized fundamental frequencies $\Omega = \omega a^2(\rho/E_2h^2)^{1/2}$ *of cross-ply moderately thick square spherical shallow shell panels,* $a/h = 10$

Panel	R/a	5	10	20	50	100	10^5
[0/90]	[22]	9·337	9·068	8·999	8·980	8·977	8·976
	[24]	9·292	9·033	8·966	8·948	8·945	8·944
	[27]	9·2509	9·0086	8·9467	8·9293	8·9268	8·9259
	[37]	9·248	9·006	8·944	8·927	8·924	8·923
	S_2	9·2008	8·9870	8·9322	8·9168	8·9145	8·9138
[0/90/0]	[22]	12·06	11·86	11·81	11·79	11·79	11·79
	[24]	12·200	12·019	11·873	11·960	11·959	11·958
	[27]	11·8149	11·6466	11·6038	11·5918	11·5901	11·5895
	[37]	11·685	11·515	11·472	11·459	11·458	11·457
	S_2	11·6713	11·5140	11·4702	11·4554	11·4523	11·4503
$[0/90]_S$	[22]	12·04	11·84	11·79	11·78	11·78	11·78
	[24]	12·208	12·026	11·980	11·967	11·965	11·965
	[27]	11·8148	11·6465	11·6038	11·5918	11·5901	11·5895
	[37]	11·811	11·642	11·599	11·587	11·586	11·585
	S_2	11·7917	11·6380	11·5958	11·5819	11·5792	11·5775

the various radius-to-curved-length ratio from $R/a = 5$ to flat plates. Material properties are the same as in Table 7. The present results checked well with traditional higher order theory of Reddy and Liu [22], Librescu *et al.* [24], Wu *et al.* [27], and Chao and Tung [37].

TABLE 10

Normalized frequencies $\Omega_{m,n} = \omega_{m,n} a^2 (\rho/E_2 h^2)^{1/2}$ *of* $[0/90]_S$ *cross-ply square spherical shallow shell panels*

R/a	a/h	m, n	1,1	1,2	2,1	2,2	1,3
3	10	$[12]^k$	12·79278	22·63890	29·72045	35·17592	38·31140
		[21]	13·05551	23·20745	30·39797	36·29395	39·79291
		S_2	12·11566	21·98095	26·97128	32·69434	37·27270
	100	[12]	47·41525	60·97662	76·26018	75·13405	86·46918
		[21]	47·95226	62·66462	78·29612	77·97635	90·59067
		S_2	45·29985	59·41826	74·82526	73·65320	85·46741
5	10	[12]	12·43619	22·36235	29·56296	35·10534	38·07252
		[21]	12·61308	22·84572	30·16340	36·15446	39·46570
		S_2	11·78305	21·71632	26·80590	32·63062	37·03740
	100	[12]	31·07907	42·92415	62·92941	65·99475	67·79810
		[21]	31·46153	44·09002	64·44392	68·43393	70·80062
		S_2	29·92289	42·17802	62·11863	65·23026	67·37816
10	10	[12]	12·28005	22·24316	29·49652	35·07542	37·97058
		[21]	12·41384	22·68744	30·06171	36·09381	39·32355
		S_2	11·63377	21·59622	26·73362	32·59945	36·93022
	100	[12]	20·38024	32·30546	56·30135	61·71514	58·08370
		[21]	20·65688	33·12916	57·49284	63·92740	60·40510
		S_2	19·94244	32·08084	55·82609	61·28186	57·94395

Same material property as in Table 7.

To show the difference between the moderately thick and thin lamination, Table 10 is presented for the first five mode natural frequencies of the $[0/90]_S$ square spherical shallow shell panels. Verification has also been made against Reddy [12] with $\kappa = \frac{5}{6}$, and Wang and Schweizerhof [21].

Cylindrical versus spherical panels: Comparison of cross-ply cylindrical and spherical curved panels for the same material, thickness, stacking sequence and curvature is made in Table 11. Normalized fundamental frequencies of the cross-ply cylindrical and spherical shell panels are examined for thickness ratio $h/a = 0{\cdot}05$, 0·10 and 0·15, and radius-to-side-ratio $R/a = 1, \ldots, 10^{30}$ with Bhimaraddi's [29] constant shear deformation (CSD or FSDT) parabolic shear deformation (PSD or HSDT), and 3-D analysis. Strictly speaking, the single-terms assumption for the three-dimensional stresses in reference [29] is to ignore the Poisson ratio effects on the stiffness in other directions, and thereby lower frequency results. A few lower CSD frequencies are noted for a reduced shear modulus by use of $\kappa = \pi^2/12$. The present frequency results are also the lower when compared to those of Leissa and Qatu's [26] elastic deformation study, Ye and Soldatos's [32] 3-D study, and Wu *et al.* [42] refined asymptotic theory.

Spherical and saddle panels: To check the effects of curvature in opposite directions, Table 12 presents the first eight modes of normalized frequencies $\Omega = \omega R_y (\rho/E_2)^{1/2}$ for the cross-ply moderately thick spherical and saddle shell panels, with $a = b = 10h$ for two to 10 layers in comparison with Huang [41]

TABLE 11

Fundamental frequencies $\Omega = \omega a(\rho/E_2)^{1/2}$ *of* [0/90] *cross-ply cylindrical and spherical shell panels*

Panel	$h/a = 0{\cdot}05$	0·10	0·15	0·05	0·10	0·15
Cylindrical		$R_y/a = 1$			$R_y/a = 10$	
$[29]^{3-D}$	0·78683	1·04085	1·29099	0·47859	0·89564	1·23374
$[29]^{PSD}$	0·79993	1·09189	1·38174	0·47997	0·90150	1·24875
$[29]^{CSD}$	0·79798	1·07475	1·33274	0·47677	0·88026	1·19342
[32]	0·79316	1·06973	1·34537	0·47959	0·89778	1·23707
[26]	0·80580	1·14313	1·54124	0·48827	0·96074	1·41709
[42]	0·79255	1·06756	1·33990	0·47941	0·89698	1·23394
S_2	0·63361	0·95501	1·24725	0·47746	0·89526	1·23350
		$R_y/a = 2$			$R_y/a = 10^{30}$	
$[29]^{3-D}$	0·57252	0·93627	1·25377	0·47635	0·89179	1·22905
$[29]^{PSD}$	0·58000	0·95664	1·28933	0·47483	0·89761	1·24437
$[29]^{CSD}$	0·57733	0·93653	1·23527	0·47161	0·87640	1·18923
[32]	0·57702	0·94951	1·27598	0·47371	0·89248	1·23001
S_2	0·52582	0·91797	1·24773	0·47279	0·89032	1·22730
Spherical		$R_y/a = 1$			$R_y/a = 10$	
$[29]^{3-D}$	1·29835	1·39974	1·51936	0·49127	0·89912	1·23249
$[29]^{PSD}$	1·32595	1·49075	1·68141	0·49341	0·90679	1·25034
$[29]^{CSD}$	1·32483	1·48008	1·64797	0·49031	0·88584	1·19559
[26]	1·33000	1·52391	1·78940	0·50149	0·96519	1·41639
[42]	1·31049	1·44004	1·58988	0·49218	0·90038	1·23232
S_2	1·27703	1·36100	1·45599	0·48953	0·89223	1·21857
		$R_y/a = 2$			$R_y/a = 10^{30}$	
$[29]^{3-D}$	0·79577	1·05528	1·31111	0·47365	0·89179	1·22905
$[29]^{PSD}$	0·81059	1·09708	1·38083	0·47483	0·89761	1·24437
$[29]^{CSD}$	0·80870	1·08054	1·33375	0·47161	0·87640	1·18923
S_2	0·78987	1·03456	1·26593	0·47336	0·89228	1·22985

$E_1/E_2 = 25$, $E_1/E_2 = 1$, $G_{12}/E_2 = G_{13}/E_2 = 0{\cdot}5$, $G_{23}/E_2 = 0{\cdot}2$, $\nu_{12} = 0{\cdot}25$, $\nu_{31} = 0{\cdot}03$, $\nu_{23} = 0{\cdot}40$, $a = b$, Cylindrical: $R_x = \infty$, a in axial direction; Spherical: $R_x = R_y = R$.

three-dimensional analysis. The present results are generally of lower frequencies except for the nine out of 160 cases compared.

3.3. ANGLE-PLY SHELL PANELS

Now, consider the angle-ply cylindrical shallow panels. Convergence of the normalized fundamental frequency of the $[\pm 45]$ cylindrical panels of shallowness angle $\phi = 20^\circ$ is firstly examined in Table 13. Both the S_2 and S_3 displacement fields have been employed. Seven terms for m, n each in the double Fourier series is

TABLE 12

First eight frequencies $\Omega = \omega R_y(\rho/E_2)^{1/2}$ for cross-ply shallow shell panels

	L	$\Omega_{1,1}$	$\Omega_{1,2}$	$\Omega_{1,3}$	$\Omega_{2,1}$	$\Omega_{2,2}$	$\Omega_{2,3}$	$\Omega_{3,1}$	$\Omega_{3,2}$
					Spherical panels, $R = 50h$, $a = b = 10h$				
[41]	2	4·6238	*10·7530	*19·1300	10·8640	14·9090	*21·9610	19·3150	22·0530
	3	5·8423	9·2156	15·3830	14·1380	15·9720	20·2920	23·1960	24·4470
	4	5·8070	*12·1340	*19·8460	12·8800	16·2980	*22·7190	19·9320	22·7570
	5	6·1090	10·9820	17·6890	14·0130	16·7910	21·8330	22·6270	24·4830
	10	6·2293	*13·0500	*21·0420	13·0760	17·4320	*24·0270	21·0820	24·0450
S_2	2	4·5945	10·7731	19·1967	10·7988	14·8856	21·9944	19·2088	21·9754
	3	5·8307	9·2070	15·3759	14·1281	15·9623	20·2830	23·1857	24·4365
	4	5·7900	12·1581	19·8987	12·1367	16·2832	22·7428	19·8526	22·7049
	5	6·0977	10·9729	17·6814	14·0042	16·7816	21·8241	22·6190	24·4739
	10	6·2163	13·0597	21·0686	13·0460	17·4215	24·0374	21·0374	24·0149
					Saddles, $R_x = -R_y = 20h$, $a = b = 10h$				
[41]	2	1·7576	4·4079	7·8545	4·4077	6·0483	8·9442	7·8545	8·9443
	3	2·1761	3·6706	6·2281	5·6001	6·2959	8·0530	9·2751	9·7134
	4	2·2040	4·8830	8·0503	4·8826	6·5145	9·1328	8·0501	9·1328
	5	2·2819	4·3602	7·1240	5·5495	6·6218	8·6675	9·0528	9·7268
	10	2·3477	5·2011	8·4692	5·2006	6·9151	9·5898	8·4689	9·5897
S_2	2	1·6213	4·2161	7·6326	4·2219	5·7487	8·5998	7·6391	8·6025
	3	2·1566	3·6661	6·2286	5·5914	6·2901	8·0495	9·2686	9·7080
	4	2·1148	4·7833	7·9451	4·7861	6·3661	8·9670	7·9486	8·9684
	5	2·2606	4·3523	7·1217	5·5404	6·6135	8·6615	9·0471	9·7198
	10	2·2961	5·1538	8·4255	5·1544	6·8480	9·5195	8·4273	9·5201

$E_1/E_2 = 25, E_3/E_2 = 1, G_{12}/E_2 = 0{\cdot}5, G_{13} = G_{12}, G_{23}/E_2 = 0{\cdot}2, \nu_{12} = \nu_{13} = \nu_{23} = 0{\cdot}25$, [0/90/0 ...]

TABLE 13

Convergence of fundamental frequencies $\Omega = \omega\, a^2(\rho/E_2h^2)^{1/2}$ of [$\pm$ 45] angle-ply thin cylindrical panels, $\phi = 20^\circ$

$n = m$	1	2	3	4	5	6	7
[6]	27·120	26·354	26·298	26·171	26·166	—	—
[14]	27·019	27·262	27·375	27·420	27·415	27·430	27·440
S_2	28·114	26·702	25·923	25·585	25·183	24·987	24·885
S_3	23·549	21·688	20·922	20·766	20·961	20·905	20·891

$\frac{E_1}{E_2} = 40$ $\quad \frac{G_{12}}{E_2} = 0{\cdot}6$ $\quad \frac{G_{23}}{E_2} = 0{\cdot}5$ $\quad \nu_{12} = 0{\cdot}25$ $\quad a/h = 20$ $\quad R_y = a/\left[2\sin\left(\frac{\phi}{2}\right)\right]$,

$\frac{E_3}{E_2} = 1$ $\quad \frac{G_{13}}{E_2} = 0{\cdot}6$ $\quad \nu_{23}^p = 0{\cdot}646$ $\quad \nu_{31} = 0{\cdot}25$ $\quad R_x = \infty$ $\quad b = R_y\,\phi$.

TABLE 14

Fundamental frequencies of antisymmetric laminated cylindrical panels of square planform

	θ	0°	30°	45°	60°	90°	0°	30°	45°	60°	90°
Layers		Shallownes angle $\phi = 30°$					Shallownes angle $\phi = 45°$				
2	[23]	19·98	23·52	36·48	50·21	56·34	22·85	31·36	51·59	53·97	56·08
	[19]	20·04	23·69	36·82	51·38	—	22·97	31·68	52·19	74·48	—
	[40]	19·11	22·12	29·22	33·51	36·58	—	—	—	—	—
	[28]	20·05	23·54	36·53	51·22	—	—	—	—	—	—
	$S_3^{\#1}$	12·66	16·51	24·84	28·91	34·38	15·85	22·65	33·56	35·03	39·71
	$S_3^{\#2}$	12·43	16·13	24·39	28·27	33·59	15·57	22·06	33·03	34·12	38·66
4	[23]	19·98	27·99	40·01	52·69	56·34	22·85	34·84	54·18	69·75	56·08
	[19]	20·04	28·16	40·32	53·61	—	22·97	35·12	54·70	76·04	—
	[28]	20·05	28·06	40·14	53·52	—	—	—	—	—	—
	$S_3^{\#1}$	12·66	18·57	28·34	32·48	34·38	15·85	24·45	36·80	39·65	39·71
	$S_3^{\#2}$	12·43	18·17	27·66	31·82	33·59	15·57	23·80	35·86	38·52	38·66
∞	[23]	19·98	29·26	41·05	53·40	56·34	22·85	35·86	54·97	71·41	56·08
	[19]	20·04	29·37	41·30	54·26	—	22·97	36·08	55·43	76·50	—
	[28]	20·05	29·37	41·30	54·26	—	—	—	—	—	—
	$S_3^{\#1}$	12·66	19·02	30·04	33·13	34·38	15·85	24·82	38·38	41·24	39·71
	$S_3^{\#2}$	12·43	18·60	29·41	32·53	33·59	15·57	24·18	37·52	40·11	38·66

$\frac{E_1}{E_2} = 40$, $G_{23} = 0{\cdot}5\ E_2$, $G_{12} = G_{13} = 0{\cdot}6E_2$ for mat. #1 in reference [40], or

$\frac{E_3}{E_2} = 1$, $\nu_{12} = \nu_{13} = \nu_{23} = 0{\cdot}25$, $G_{12} = G_{13} = 0{\cdot}5E_2$ for mat. #2 in references [23, 19, 28].

enough to attain good convergence, and the present results are considerably lower than those of Soldatos [6], and Kabir and Chaudhuri [14].

To show the effects of number of layers, shallowness angles and fiber orientations, the normalized fundamental frequencies $\Omega = \omega b^2 (\rho/E_2 h^2)^{1/2}$ are shown in Table 14 for the antisymmetric laminated cylindrical panels with thickness ratio fixed at $a/h = 20$, number of layers from 2 to infinity, shallowness angle $\phi = 30°$ and 45°, and fiber orientations $\theta = 0°, 30°, 45°, 60°$ and 90°. By use of the S_3 displacement fields, a good comparison has been done with Soldatos [23], Mizusawa and Kito [19], Huang and Dasgupta [40], and Mizusawa [28] in which an HSDT-based spline strip method was used. The present results are remarkably lower than all of theirs. However, reference [40] was the closest correspondence as a result of the same three-dimensional point of view in spite of different solution methods. In the case of angle-ply, the S_3-type displacement field is used because of its suitability for tangential movement along the edges.

3.4. VARIOUS PANEL CONFIGURATION

In an overview that follows, a series of various doubly curved shallow shell panels is discussed for the effects of stacking sequence, geometrical

TABLE 15

Normalized frequencies $\Omega = \omega a^2 (\rho/E_2)^{1/2}$ *of simply supported* $[0/90]_S$ *symmetric cross-ply square shell panels*

	a/h		Ω_1	Ω_2	Ω_3	Ω_4	Ω_5	Ω_6
Saddle panels	10	S_2	15·0152	25·8072	36·9498	42·4362	42·7485	54·6470
($R_x = 10a$)	20	S_2	17·5349	31·0719	53·6994	56·3848	60·1950	77·1561
($R_y = -R_x$)	50	S_2	18·4014	33·5264	64·5347	65·4062	72·0046	92·0230
	100	S_2	18·0302	34·8389	67·5922	68·3070	74·2883	95·0335
Plate	10	S_1	15·0627	25·8320	36·9729	42·4430	42·7826	54·6770
($a/R_x = 0$)		S_2	15·0627	25·8317	36·9734	42·4446	42·7829	54·6787
($a/R_y = 0$)	20	S_1	17·6142	31·0762	53·7147	56·3474	60·2510	77·2077
		S_2	17·6141	31·0758	53·7147	56·3461	60·2508	77·2069
	50	S_1	18·6412	33·2877	64·0629	65·2851	72·1219	92·1039
		S_2	18·6412	33·2876	64·0624	65·2851	72·1219	92·1036
	100	S_1	18·8052	33·6468	65·4766	67·6665	74·5650	95·1267
		S_2	18·8052	33·6468	65·4764	67·6665	74·5650	95·1266
Cylindrical	10	S_2	15·0·711	25·8375	36·9844	42·4536	42·7877	54·6859
panels	20	S_2	17·6549	31·0918	53·7662	56·3671	60·2675	77·2247
($a/R_x = 0$)	50	S_2	18·8856	33·3193	64·1098	65·6326	72·2049	92·1600
($R_y = 10a$)	100	S_2	19·7216	33·6410	65·5115	69·0583	74·8481	95·2509
Spherical	10	S_2	15·1067	25·8789	36·9851	42·4931	42·7819	54·6921
panels	20	S_2	17·8237	31·2739	53·7903	56·5250	60·3032	77·2655
($R_x = 10a$)	50	S_2	19·9592	34·4771	65·0891	65·8382	72·4760	92·4575
($R_y = 10a$)	100	S_2	23·6321	38·0870	69·3475	69·9023	75·9559	96·4634

$E_1/E_2 = 40$, $E_3/E_2 = 1$, $G_{12}/E_2 = 0{\cdot}6$, $G_{13}/E_2 = 0{\cdot}6$, $G_{23}/E_2 = 0{\cdot}5$, $\nu_{12} = \nu_{13} = 0{\cdot}25$, $\nu_{23}^p = 0{\cdot}641$.

configuration, curvatures in opposite directions, thickness, and type of boundary conditions.

Symmetric cross-ply: As a typical example, comparison of natural frequencies is made for the various shaped moderate thick to thin symmetric $[0/90]_S$ cross-ply curved panels of square planform. For ease of normal movements along edges, typically S_2 boundary condition and displacement fields are employed in numerical computation. Results of S_1 fixed pin supports are also given for the plates with only slight difference. Increasing frequencies are noted for the first six modes in Table 15 in the order of saddle, plate, cylindrical and spherical shallow shells in accordance with the minimum total potential energy principle for the various geometrical configurations.

Symmetric angle-ply: In a final example, natural frequencies are discussed in Table 16 for the first few modes of the simply supported $[45/-45]_S$ symmetric angle-ply square plan form curved panels from moderate to thin thickness. Both S_2 and S_3-type edge boundary conditions and displacement fields have been used for the saddle, plate, cylindrical and spherical panels. It is noted that natural frequencies are to increase in the same order as the cross-ply above. S_3 is the most suitable for angle-ply of the all except for the spherical shapes for which the S_2 functions are preferred.

TABLE 16

Normalized frequencies $\Omega = \omega a^2(\rho/E_2 h^2)^{1/2}$ *of simply supported* $[45/-45]_S$ *symmetric cross-ply square shell panels*

	a/h		Ω_1	Ω_2	Ω_3	Ω_4	Ω_5	Ω_6
Saddle panels	10	S_2	18·0360	31·6922	34·4834	37·0465	45·4222	55·1545
($R_x = 10a$)		S_3	17·6441	29·7159	31·1708	33·1842	40·5254	42·4109
($R_y = -R_x$)	20	S_2	21·5486	40·3099	51·2038	63·0031	68·9320	78·2848
		S_3	21·1111	37·5716	40·7966	53·5785	58·3716	67·4669
	50	S_2	22·9140	44·9756	60·0334	73·7082	94·1282	107·9297
		S_3	23·7443	42·7873	49·9326	68·0441	68·9959	100·4039
	100	S_2	22·6762	47·1488	62·7339	76·0074	98·1066	112·8214
		S_3	27·4665	46·1189	57·5584	72·6650	81·1309	107·3599
Plate	10	S_2	18·1058	31·6761	34·4144	37·0320	45·4613	55·1427
($a/R_x = 0$)		S_3	17·6039	29·6919	31·1450	33·2055	40·5107	42·3885
($a/R_y = 0$)	20	S_2	21·6397	40·2410	51·1496	63·0426	68·8288	78·2469
		S_3	20·9239	37·4726	40·6969	53·5054	58·4180	67·4189
	50	S_2	23·1467	44·5100	59·6856	73·6734	93·8869	107·8227
		S_3	22·5476	42·1739	49·3665	67·6315	68·8182	100·1561
	100	S_2	23·3941	45·2554	61·3201	75·7078	97·1051	112·3018
		S_3	22·9831	43·7250	55·5288	71·8643	79·7067	106·5833
Cylindrical	10	S_2	18·2143	31·6961	34·4334	37·0448	45·4942	55·1497
panels		S_3	17·8522	29·7822	31·1813	33·1944	40·5325	42·4306
($a/R_x = 0$)	20	S_2	22·0656	40·3213	51·2065	63·1524	68·8575	78·2785
($R_y = 10a$)		S_3	21·8549	37·8363	40·8567	53·6030	58·5447	67·4303
	50	S_2	25·6465	44·9783	60·0457	74·2823	94·0702	108·1129
		S_3	27·7457	44·3836	50·7089	68·4070	69·7206	100·4897
	100	S_2	32·2080	46·9165	62·8222	77·9935	97·7917	113·3822
		S_3	39·7804	51·9084	61·8761	75·3627	83·4225	108·5618
Spherical	10	S_2	18·6050	31·7243	34·4145	37·0601	45·6179	55·1470
panels	20	S_2	23·3875	40·4617	51·3005	63·4847	68·8291	78·3018
($R_x = 10a$)	50	S_2	32·2629	45·9105	60·7028	75·9478	94·2987	108·7782
($R_y = 10a$)	100	S_2	50·6093	50·7432	65·3232	83·7801	98·7530	115·9839

Note: Same geometry and material properties as in Table 15.

4. CONCLUSIONS

1. A complete survey of the literature has been conducted and comparison with it made on free vibration of composite laminated shallow shell panels according to the present three-dimensional theory. Lowest frequencies are obtained in the order of saddle (hyperbolic), flat plate, cylindrical and spherical configurations in accordance with the minimum total potential energy.
2. The present three-dimensional semi-analytical solution is based on the theory of elasticity. Unlike the traditional theories of plates and shells, the 3-D boundary conditions and interlaminar continuity of layer displacements and

transverse stresses are satisfied by use of the assumed admissible displacement fields and Lagrange's multipliers via a 3-D augmented energy variational approach to the natural state.

3. A system of three-dimensional higher order displacement fields has been developed for a variety of edge boundary conditions such as S_1 fixed pin, S_2 hinge-roller, and S_3 sliding pin supports in consistence with physical reality and mathematical requirements. Cases other than simply supported will be treated in follow up papers.
4. In general, the S_2 displacement functions are most suitable for cross-ply and S_3 for angle-ply curves panels for ease of normal and tangential movements along edges, respectively. In certain circumstances of symmetric angle-ply thin spherical panels, edgewise sliding is likely to be hindered by the double curvature, and the S_2 displacement functions are preferred for lower frequencies.

ACKNOWLEDGMENTS

This work is supported by the National Science Council of the Republic of China through grant NSC86-2212-E-007-007.

REFERENCES

1. J. M. Deb Nath 1969 *Ph.D. Dissertation, University of Southampton.* Dynamics of rectangular curved plates
2. R. D. Blevins 1979 *Formulas for Natural Frequency and Mode Shape.* Fl Krieger.
3. W. Soedel 1981 *Vibration of Sheels and Plates.* New York: Marcel Dekker.
4. N. S. Bardell and D. J. Mead 1989 *Journal of Sound and Vibration* **134**, 29–54. Free vibration of an orthotropic stiffened cylindrical shell, Part I: discrete line simple supports.
5. Y. Kobayashi and A. W. Leissa 1995 *International Journal of Non-Linear Mechanics* **30**, 57–66. Large amplitude free vibration of thick shallow shells supported by shear diaphragms.
6. K. P. Soldatos 1983 *Quarterly Journal of Mechanics and Applied Mathematics* **36**, 207–221. Free vibration of antisymmetric angle-ply laminated circular cylindrical panels.
7. P. C. Shen and J. G. Wan 1987 *Computers and Structures* **25**, 1–10. Vibration analysis of flat shells by using B spline functions.
8. G. N. Geannakakes and P. C. Wang 1991 *Computers and Structures* **39**, 489–492. Vibration analysis of arbitrarily-shaped shell panels using B_3-spline finite strips.
9. S. C. Fan and M. H. Luah 1995 *Journal of Sound and Vibration* **179**, 763–776. Free vibration analysis of arbitrary thin shell structures by using spline finite element.
10. P. K. Sinha and A. K. Rath 1975 *Aeronautical Quarterly* **26**, 211–218. Vibration and buckling of cross-ply laminated circular cylindrical panels.
11. C. Bert and M. Kumar 1982 *Journal of Sound and Vibration* **81**, 107–121. Vibration of cylindircal shells of bimodulus composite materials.
12. J. N. Reddy 1984 *ASCE Journal of Engineering Mechanics* **110**, 794–809. Exact solutions of moderately thick laminated shells.
13. H. Fong 1984 *Eight U.S. General Purpose Programs, in Structural Mechanics Software Series*, (N. Perrone *et al.* editors) Vol. 5, 125–156. Charlottesville, VA. University Press of Virginia.

14. H. R. H. Kabir and R. A. Chaudhuri 1991 *International Journal of Solids Structures* **28**, 17–32. Free vibration of shear-flexural antisymmetric angle-ply doubly curved panels.
15. M. Ganapathi, T. K. Varadan and V. Balamurugan 1994 *Computers and Structures* **53**, 335–342. Dynamic instability of laminated composite curved panels using finite element method.
16. D. Chakravorty, J. N. Bandyopadhyay and P. K. Sinha 1995 *Journal of Sound and Vibration* **181**, 43–52. Finite element free vibration analysis of point supported laminated composite cylindrical shells.
17. D. Chakravorty, J. N. Bandyopadhyay 1995 *Computers and Structures* **54**, 191–198. Free vibration analysis of point-supported laminated composite doubly curves shells—a finite element approach.
18. S. Goswami and M. Mukhopadhyay 1995 *Journal of Composite Materials* **29**, 2388–2422. Finite element free vibration analysis of laminated composite stiffened shell.
19. T. Mizusawa and H. Kito 1995 *Computers and Structures* **56**, 589–604. Vibration of angle-ply laminated cylindrical panels by the spline strip method.
20. T. Mizusawa and H. Kito 1995 *Computers and Structures* **57**, 253–265. Vibration of cross-ply laminated cylindrical panels by the spline strip method.
21. J. Wang and K. Schweizerhof 1996 *International Journal of Solids and Structures* **33**, 11–18. Boundary-domain element method for free vibration of moderately thick laminated orthotropic shallow shells.
22. J. N. Reddy and C. F. Liu 1985 *International Journal of Enginnering, Science* **23**, 319–330. A higher-order shear deformation theory of laminated elastic shells.
23. K. P. Soldatos 1987 *Journal of Sound and Vibration* **119**, 111–137. Influence of thickness deformation on free vibrations of rectangular plates, cylindrical panels and cylinders of antisymmetric angle-ply construction.
24. L. Librescu, A. A. Khdeir and D. A. Frederick 1989 *Acta Mechanica* **76**, 1–33. Shear deformable theory of laminated composite shallow shell-type panels and their response analysis I: free vibration and buckling.
25. A. N. Palazotto and P. E. Linnemann 1991 *International Journal of Solids and Structures* **28**, 341–361. Vibration and buckling characteristics of composite panels incorporating the effects of a higher order shear theory.
26. A. Leissa and M. S. Qatu 1991 *ASME Journal of Applied Mechanics* **58**, 181–188. Equations of elastic deformation of laminated composite shallow shells.
27. C. P. Wu, K. W. Tseng and L. C. Kuo 1995 *Journal of Chineses Society of Mechanical Engineers* **16**, 221–237. Vibration and stability of simply supported cross-ply double curved shells.
28. T. Mizusawa 1996 *Computers and Structures*, **61**, 441–457. Vibration of thick laminated cylindrical panels by the spline strip method.
29. A. Bhimaraddi 1991 *International Journal of Solids and Sturctures* **27**, 897–913. Free vibration analysis of doubly curves shallow shells on rectangular planform using three-dimensional elasticity theory.
30. J. Fan and J. Zhang 1992 *ASCE Journal of Engineering Mechanics* **118**, 1338–1356. Analytical solutions for thick, doubly curved, laminated shells.
31. A. Beakou and M. Touratier 1993. *International Journal for Numerical Methods in Engineering* **36**, 627–653. A rectangular finite element for analysing composite multilayered shallow shells in statics, vibration and buckling.
32. J. Q. Ye and K. P. Soldatos 1994 *Composite Engineering* **4**, 429–444. Three dimensional vibration of laminated cylinders and cylindrical panels with symmetric or antisymmetric cross-ply lay-up
33. T. P. Philippidis 1994 *Journal of Composite Materials* **28**, 252–261. The transverse Poisson's ratio in fiber reinforced laminae by means of a hybrid experimental approach.

34. C. C. Chao and T. P. Tung 1992 *Localized Damage* '92, 327–346. Southampton, U.K.: Computational Mechanics Publishers. A three-dimensional consistent higher-order laminated shell theory and impact damage prediction.
35. C. C. Chao, T. P. Tung, C. C. Sheu and J. H. Tseng 1994 *ASME Journal of Vibration and Acoustics* **116**, 371–378. A consistent higher-order theory of laminated plates with nonlinear impact modal analysis.
36. C. C. Chao, T. P. Tung and H. H. Li 1994 *ASME Journal of Energy Resources Technology* **116**, 240–249. 3-D stress analysis of cross-ply laminates.
37. C. C. Chao and T. P. Tung 1995 *Composite Engineering* **5**, 297–312. Consistent higher-order analysis on shock response of cross-ply curved panels.
38. C. C. Chao and C. Y. Tu 1999 *Composite*: *Part B Engineering* **30B**, 9–22. Three-dimensional contact dynamics of laminated plates: Part 1. Normal Impact.
39. C. Y. Tu and C. C. Chao 1999 *Composites*: *Part B Engineering* **30B**, 23–41. Three-dimensional contact dynamics of laminated plates: Part 2. Oblique impact with friction.
40. K. H. Huang and A. Dasgupta 1995 *Journal of Sound and Vibration* **186**, 207–222. A layer-wise analysis for free vibration of thick composite cylindrical sheels.
41. N. N. Huang 1995 *Acta Mechanica* **108**, 23–34. Exact analysis for three dimensional free vibrations of cross-ply cylindrical and doubly-durved laminates.
42. C. P. Wu, J. Q. Tarn and S. C. Tang 1998 *International Journal of Solids Structures* **35**, 1953–1979. A refined asymptotic theory for dynamic analysis of doubly curved laminated shells.